Journal of Electrical Engineering, Vol. 74, No. 6, 2023, pp. 492-502

sciendo

PAPERS

A virtual synchronous generator control method in microgrid with vehicle-to-grid system

Van Tan Nguyen, Hong Viet Phuong Nguyen*, Thi Bich Thanh Truong, Quang Vu Truong

The inertia in power systems plays a very important role in stabilizing the power system. With the growth of distributed generation (DG)/renewable energy source (RES) penetration in the power grid, there has been a concern about the lack of inertia in the power system. One of the solutions to solve the problem is to use the Virtual Synchronous Generator (VSG) control method. For energy storage, the Vehicle-to-grid (V2G) storage system can replace the traditional hybrid energy storage which consists of batteries and supercapacitors. This application will be implemented in Microgrid. The article will focus on simulating the Microgrid with the V2G system and solar energy as a renewable energy source, the inverters are controlled by the method of VSG control. The models will be simulated and the results will be shown on MATLAB/SIMULINK software.

Keywords: renewable energy, V2G, microgrid, virtual synchronous generator, power system stability

1 Introduction

Traditional electricity sources such as thermal power, coalfired power, and oil-fired power plants typically supply electricity directly to the distribution grid through synchronous generators. This creates a large rotational inertia due to the rotating turbines of the generators, which helps to stabilize the grid frequency promptly during emergencies or changes in demand [1]. However, traditional energy sources are causing significant environmental impacts on the living environment of residents and organisms on Earth due to the large amount of carbon emissions released into the atmosphere. Additionally, the supply of coal and oil is limited. To deal with this situation, renewable energy is becoming an effective solution to reduce the impact of traditional energy sources and ensure a sustainable energy supply in the future.

Microgrid consists of elements such as small power sources, distributed generators, storage systems, and loads [2]. With the self-supply characteristics of Microgrid, distributed energy, especially solar energy, plays an essential role in Microgrid [2]. However, unlike traditional energy sources, Distributed Generation (DG)/Renewable Energy Source (RES) units have either very small or no rotating mass (low inertia) and damping property [3]. Furthermore, DG/RES also has an inconsistent power quality due to the unstable output power caused by external factors such as weather, and solar radiation, etc. which has resulted in stability and reliability problems. These disadvantages make it challenging to integrate distributed energy sources into independent or distri-bution grids.

In order to address the difficulties of renewable power sources connected to the grid, the concept of adding virtual inertia is being developed in many researches [3-7]. One of those concepts is by using the VSG control method for a voltage-sourced converter (VSC) with an energy storage system (ESS) [3]. A VSC can create virtual inertia by simulating the working characteristics of the synchronous generator (SG) to convert the power electronics into a virtual synchronous generator (VSG) [3, 8-10]. The VSG dynamic circuit model includes an energy storage system, the VSC controlled by VSG control method [3]. Therefore, the distributed energy generator can be operated like a synchronous generator to contribute to stabilizing the grid frequency.

Regarding energy storage systems, energy storage measures such as batteries, supercapacitors, or flywheels are very expensive to invest in, so instead of using these energy storage systems, electric vehicles (EVs) of consumers are considered as a replacement [2]. The vehicle-to-grid (V2G) technology is feasible because of the large energy storage capacity of electric vehicles (which are increasingly being used) and electric vehicles are often in an unused state for long periods, specifically 96% of the time, such as when parked in public car parks or at home [11-12]. Utilizing consumer electric vehicles as part of the energy storage system reduces the investment cost in other storage systems as well as increases the stability of the energy storage system. With these advantages, the V2G system can become an essential component of the energy system in the future.

Researchers and industry experts are actively exploring the role of electric vehicles (EVs) in frequency regulation strategies, primarily focusing on large-scale

Faculty of Electrical Engineering, The University of Danang – University of Science and Technology, Da Nang, Vietnam
*nhvphuong@dut.udn.vn

https://doi.org/10.2478/jee-2023-0057, Print (till 2015) ISSN 1335-3632, On-line ISSN 1339-309X

power systems. Studies like [2, 13] have proposed control strategies that enable EVs to respond to automatic generation control (AGC) signals from the power grid, facilitating their participation in frequency adjustment. In addition to these control strategies, researchers are also investigating the underlying battery technology that will enable EVs to participate in frequency regulation [14], while [15] surveys the bidirectional DC-DC converters for EV battery systems.

In this paper, the control methods will be investigated to turn electric vehicles (EVs) into virtual synchronous generators (VSG), in order to assist in frequency and voltage stabilization for islanded Microgrid. The paper is organized as follows: Sect.II introduces the Microgrid structure and its components. Sect.III depicts the principle of VSG control method. Sect.IV presents the control scheme for the ESS of EVs. Sect.V shows the power calculation of V2G system. Simulation results are shown in Sect.VI. Finally, Sect.VII concludes this research.

2 Microgrid scheme with vehicle-to-grid system

Figure 1 shows the structure of MG. In this paper, MG operates in islanded mode and is divided into two sectors DC and AC. The two sides are connected by VSC DC/AC controlled by the VSG method.

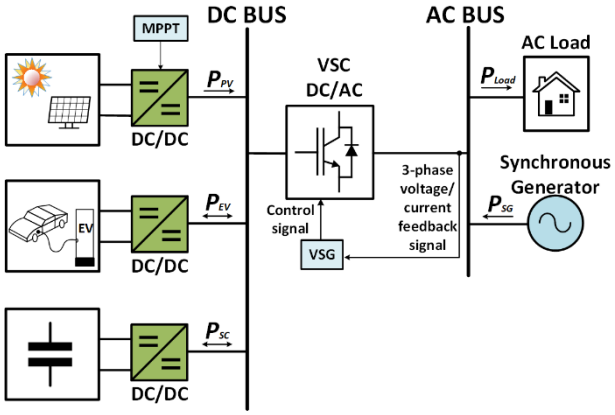

Fig. 1. Structure diagram of a microgrid with EVs

On the DC side, there are PV solar systems, electric vehicles, and supercapacitors (SC). The DC/DC converter at the DG side is a boost converter controlled by pulse signals from the MPPT algorithm [16]. P&O is chosen as an MPPT algorithm for this research because of its simplicity and can be applied to all PV systems [17]. The other DC/DC converter is a bidirectional buck/boost converter. On the AC side, there are AC loads and a synchronous generator. The role of the synchronous generator in the Microgrid is to be a backup generator and partly participate in the primary frequency control process when load fluctuations happen, especially in the case when there is not enough power system present from electric vehicles.

2.1 Electric vehicles as hybrid storage systems

Nowadays, batteries are commonly used as a power source for electric vehicles [14]. According to [14], EVs in the future will be likely to pair batteries with supercapacitors since they can extend the battery life in the case of high-power pulses effect and fluctuating load.

Figure 2 shows the energy storage structure of an electric vehicle. Therefore, the storage system investigated and simulated is Hybrid Energy Storage System (HESS). Both power storage units are connected to bidirectional DC/DC converters, and each branch of the storage unit is connected in parallel to the DC bus. From the DC bus, the output power of the hybrid storage system is converted through the inverter, an electric drive for the EVs to operate. This is a simple structure design, with high flexibility and stability, capable of redundancy whenever one of the two source units fails. EVs are charged from the grid or discharged into the grid to support power.

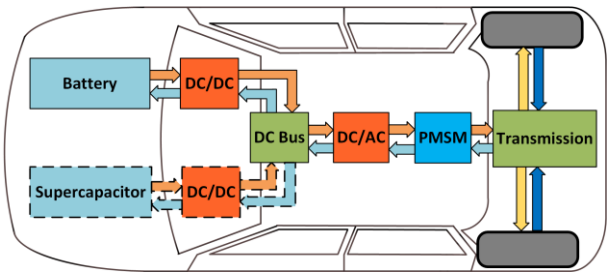

Fig. 2. Energy storage in an electric vehicle and its power flow

2.2 Bidirectional DC/DC converter

The DC/DC converter, also known as bidirectional half-bridge converter (BHBC) is responsible for controlling the bidirectional current of the storage system, and keeping the DC voltage the same at the DC bus [18]. The non-isolated converter is chosen because it is cheaper and has fewer components than the isolated type [15].

The mathematical model of the Buck-Boost converter is defined as

$$\frac{di_{ESS}}{dt} = \frac{1}{L_{ESS}} v_{ESS} - \frac{R_{ESS}}{L_{ESS}} i_{ESS} - \frac{u}{L_{ESS}} v_{DC} \quad (1)$$

where i_{ESS}, v_{ESS}, v_{DC}, R_{ESS}, L_{ESS}, u represent the input

current, input voltage, output voltage, input inductance, input resistor and duty cycle of IGBTs respectively. With Laplace transformation, Eqn. (1) becomes

$$\frac{I_{ESS}(s)}{V_{ESS}(s) - uV_{DC}} = \frac{1}{L_{ESS}s + R_{ESS}}. \quad (2)$$

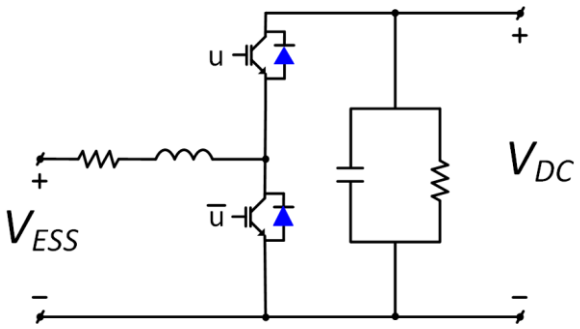

Fig. 3. Bidirectional DC/DC converter in a hybrid storage system

2.3 Three-phase voltage-sourced converter

Electric energy from the DC bus is passed to AC bus through a three-phase VSC as shown in Fig. 1. In Fig. 4, there are AC side resistors R_f, and AC side inductors L_f connected in series. V_{ta},V_{tb},V_{tc} are three-phase output voltages of the VSC. V_{sa}, V_{sb}, V_{sc} are AC system voltages in the VSC system.

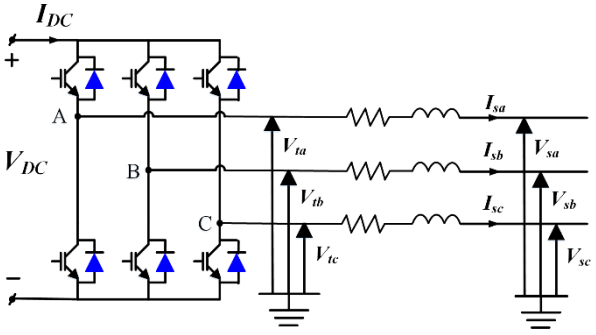

Fig. 4. Schematic diagram of a three-phase VSC

From the schematic of Fig. 4, the mathematical model of VSC output would be [19]:

$$L\frac{d\vec{i}}{dt} = -R\vec{i} + \overrightarrow{V_t} - \overrightarrow{V_s} \quad (3)$$

where $\vec{i}$, $\overrightarrow{V_t}$, $\overrightarrow{V_s}$ represent the space-phasor of the three-phase output current, terminal voltage, AC system voltage, respectively. The model (3) could be expressed in dq-frame with $\theta = \omega_0 t + \theta_0$ as

$$L\frac{di_d}{dt} = L\omega_0 i_q - Ri_d + V_{td} - V_s cos(\omega_0 t + \theta_0 - \theta)$$
$$L\frac{di_q}{dt} = L\omega_0 i_d - Ri_q + V_{tq} - V_s sin(\omega_0 t + \theta_0 - \theta) \quad (4,5)$$

in which, according to [19], V_{td} and V_{tq} are

$$V_{td}(t) = \frac{V_{DC}}{2} m_d(t) \quad (6)$$

$$V_{tq}(t) = \frac{V_{DC}}{2} m_q(t) \quad (7)$$

where $m_d(t)$ and $m_q(t)$ are modulating signals in the dq-frame. Therefore, we can control the terminal voltage by the modulating signal. Equations (6) and (7) represent the VSC model in dq-frame.

3 Principle of virtual synchronous generator technique

The idea of the VSG concept is producing the dynamic properties of a real synchronous generator (SG) for power electronics-based DG/RES units [3]. From Fig. 5, the VSG concept consists of distributed energy resources (DER) (such as wind, and solar energy), energy storage, voltage-sourced converter with a control method. Because of VSG's characteristic SG mimic, the large-scale grid stability control method and theory can be applied to control Microgrid with high penetration of DG/RES units [8]

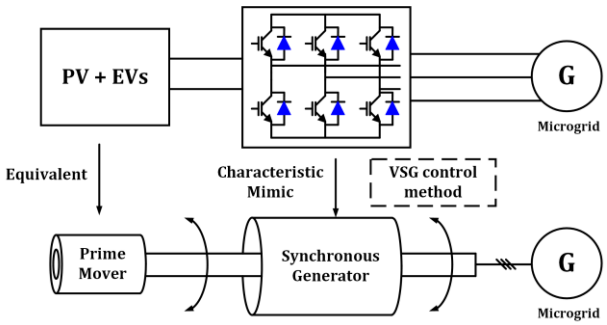

Fig. 5. Concept of virtual synchronous generator

There are two important aspects of the VSG method: mathematical modeling and control scheme. Mathematical modeling of VSG is classified into two types: high-order and low-order [20]. In this paper, a second-order model is adopted since it is commonly used in applications. This low-order model has two parts mechanical part and an electrical part presented in the equations below.

$$\begin{cases} J\omega \dfrac{d(\omega-\omega_N)}{dt} = P_m - P_e - D(\omega-\omega_g) \\ \dot{E} = \dot{U} + \dot{I}(r_a - jx_a) \\ \dfrac{d(\theta)}{dt} = \omega_0 \end{cases} \quad (8)$$

where P_m is the mechanical active power, P_e stands for the electrical active power, ω_N is the reference angular frequency, ω_0 denotes the generator's rotating speed, ω_g is the angular frequency of the grid, θ is the generator electric angle, D is the damping constant, J is the rotor inertia, r_a represents the armature resistance, x_a stands for the synchronous reactance, $\dot{U}$ is the synchronous generator output voltage, $\dot{E}$ is the induced voltage and $\dot{I}$ is used for denoting the stator current [8]. $\dot{U}$, $\dot{E}$, $\dot{I}$ values can also be expressed in dq-frame.

To determine the reference mechanical active power for VSC to exchange power with AC bus, a *P-f* droop control is implemented. P_m is computed as follows [10]:

$$\omega_g = \omega_N + D_p(P_N - P_m) \quad (9)$$

where P_N is nominal active power; D_p is damping constant in *P-f* droop control. In order to calculate the output voltage of the synchronous generator, a *Q-U* droop control is also implemented. Magnitude of $\dot{E}$ is computed as follows [10]:

$$E = U_N + D_q(Q_N - Q_{VSG}) \quad (10)$$

where D_q is the reactive power droop gain, U_N is the voltage reference, Q_N is the reactive power reference, and Q_{VSG} is the VSG output reactive power. According to [10], the electric potential can be defined in the static dq -frame, where the angle is determined in (8):

$$\dot{E} = E_d + jE_q = E\cos(\theta) + jE\sin(\theta) \quad (11)$$

From there, the $\dot{U}$ or u_o^* can be determined by Virtual Impedance mathematical model from the second equation of (8), and can be expressed in dq-frame:

$$\dot{U} = U_d + jU_q \quad (12)$$

From the mathematics equations and models above, a detailed control scheme of VSG has been compiled as shown in Fig. 6. Assuming line impedance, the state equation of the circuit can be expressed as in [8]:

$$\begin{cases} \dfrac{di_{ld}}{dt} = \dfrac{-R_f}{L_f} i_{ld} + \omega_0 i_{lq} + \dfrac{1}{L_f} v_{id} - \dfrac{1}{L_f} v_{od} \\ \dfrac{di_{lq}}{dt} = \dfrac{-R_f}{L_f} i_{lq} - \omega_0 i_{ld} + \dfrac{1}{L_f} v_{iq} - \dfrac{1}{L_f} v_{oq} \\ \dfrac{dv_{od}}{dt} = \omega_0 v_{oq} + \dfrac{1}{C_f} i_{ld} - \dfrac{1}{C_f} i_{od} \\ \dfrac{dv_{oq}}{dt} = -\omega_0 v_{od} + \dfrac{1}{C_f} i_{lq} - \dfrac{1}{C_f} i_{oq} \end{cases} \quad (13)$$

where R_f, L_f and C_f are the line parameters. From Eqn.s (4), (5), and (13), the control block diagram of VSC is represented in Fig. 7 [5, 21]. Both control loops choose PI as the controller because the PI controller is sufficient to ensure DC command following with a satisfactory performance [19]. With this VSG control method, the inertia of a Microgrid can now be calculated as shown [22]:

$$H_{sys} = \frac{\sum \frac{J_{SG}\omega_e^2}{2} + \sum \frac{J_V \omega_e^2}{2}}{S_{sys}} \quad (14)$$

4 Control strategy for energy storage system

The energy storage system consisting of batteries in EVs and super-capacitors is connected to the microgrid through bidirectional DC/DC converters and a three-phase DC/AC VSC. Therefore, a control scheme needs to be developed for enabling the converter to operate as intended and provide the desired output. The three-phase DC/AC VSC control scheme is already mentioned in Section 3. In this paper, the selected control scheme for the bidirectional DC/DC converters will be controlling V_{DC} and I_{ESS}. The control scheme is shown in Fig. 8.

4.1 Energy storage current controller

As shown in Fig. 9, the storage current consists of battery current and supercapacitor current and they are regulated by a PI controller. In feedback control, the output of the plant model is fed back and compared to the setpoint current. The error term of two values will be used by a PI controller to calculate the V_{DC} voltage. From there, I_{ESS} will be produced from the mathematical plant model, which is a bidirectional DC/DC converter.

4.2 DC voltage controller

In Fig. 10, the DC voltage is also controlled by a PI controller that calculates the reference current value of the storage system using the error between the DC voltage and its reference value. Then, the reference storage system current value will be used in the HESS block to determine the actual storage system current [23]. The relation between V_{DC} and I_{ESS} linear. The transfer function of V_{DC} and I_{ESS} is expressed as

$$\frac{V_{DC}}{I_{ESS}} = \frac{1}{\frac{C_{DC}R_{DC}}{2}s + 1}. \quad (15)$$

The transfer function is the plant model of the DC-link including capacitor and resistor to smooth the DC voltage.

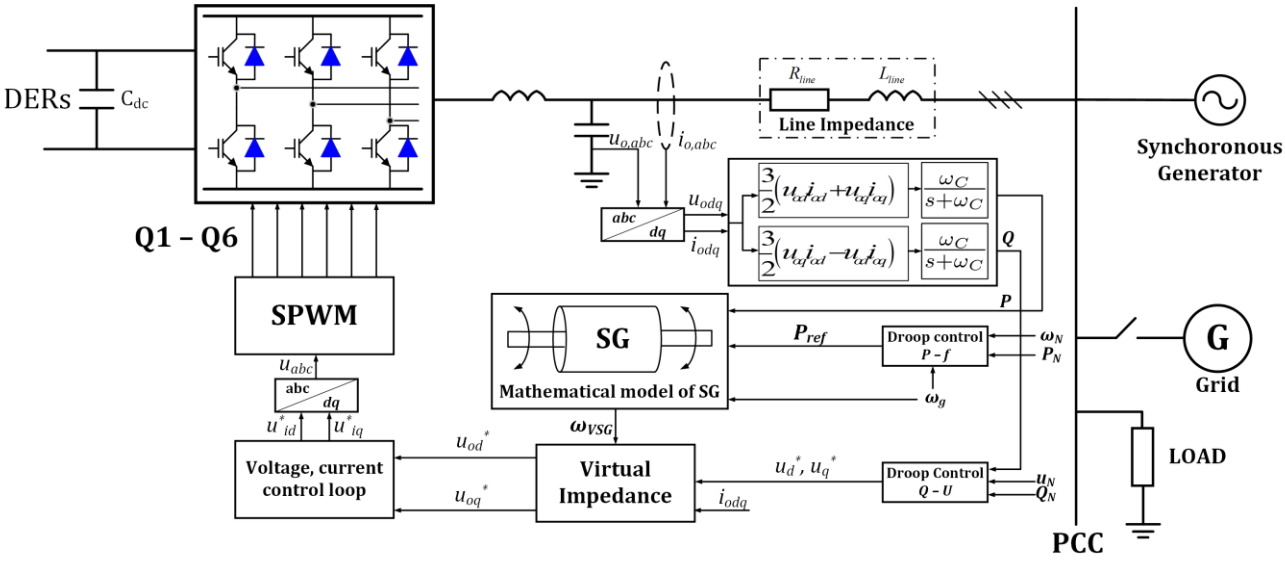

Fig. 6. Concept of virtual synchronous generator

In order to get control signals to the DC/DC units of the two storage devices, the V_{DC} voltage controller needs

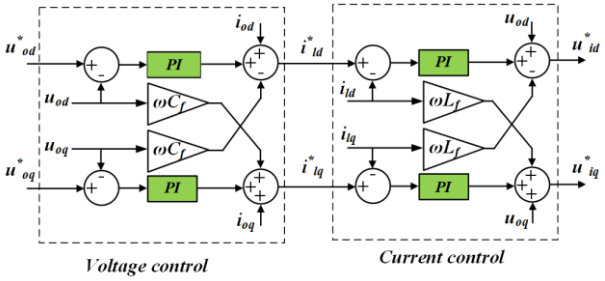

Fig. 7. Cascade control block diagram of VSC

to give them reference current signals as in Fig. 10. By using a low-pass filter, the reference current values will be divided between the battery system in the battery system (low-pass filter) and the supercapacitor system [23]. For low-pass filters, low and medium-frequency power oscillator signals (small $\Delta P/\Delta t$) are given as a reference for the battery system. In contrast, the high-frequency fluctuations signals are given as a reference for the supercapacitor system in case of the high rate of change of load power (large $\Delta P/\Delta t$). Figure 11 shows the reference current split for a hybrid storage system using a low-pass filter block. The two blocks of ESS current control in Fig. 11 are shown in detail in Fig. 9 [23].

5 V2G power calculation

5.1 Energy storage in EVs

According to [24], a proposed method for calculating the capacity and power that an electric vehicle (EV) station should provide to the grid is shown in (16). The station's storage capacity for vehicles may vary depending on the station space, but only EVs with state of charge (SoC) levels between 20% and 80% are eligible for supporting the grid. The capacity that the station can provide, considering n vehicles with their respective SoC levels, is determined by the following formula:

$$\Psi_{(n)EV}^{Avl} = \sum_{i=1}^{n} \Psi_{EV(i)}^{Avl} = \sum_{i=1}^{n} (\Psi_{Ev(i)}^{T} \times SoC_{EV(i)} \quad (16)$$

where $\Psi_{Ev(i)}^{T}$ and $SoC_{EV(i)}$ are the rated capacity and SoC of one EV, respectively. The power that a vehicle must supply to the grid is [2]

$$P_{EV(i)}^{*} = \frac{\Psi_{EV(i)}^{Avl}}{\Psi_{(n)EVs}^{Avl}} P_{(inv)}^{*} \quad (17)$$

where $P_{(inv)}^{*}$ is the required V2G power for the grid.

5.2 Supercapacitor and battery

The capacitance of a SC is calculated under worst-case scenarios so that the SC can provide sufficient instantaneous energy within the response time t (seconds). The equation for calculating the capacitance of SC system is expressed as follows [25]:

$$C_{sc} = \frac{2\Delta E_{sc}}{V_{scmax}^2 - V_{scmin}^2}, \quad (18)$$

where V_{scmax} and V_{scmin} respectively represent the maximum and minimum voltage values that a SC can safely operate at. To ensure efficiency and safe operation,

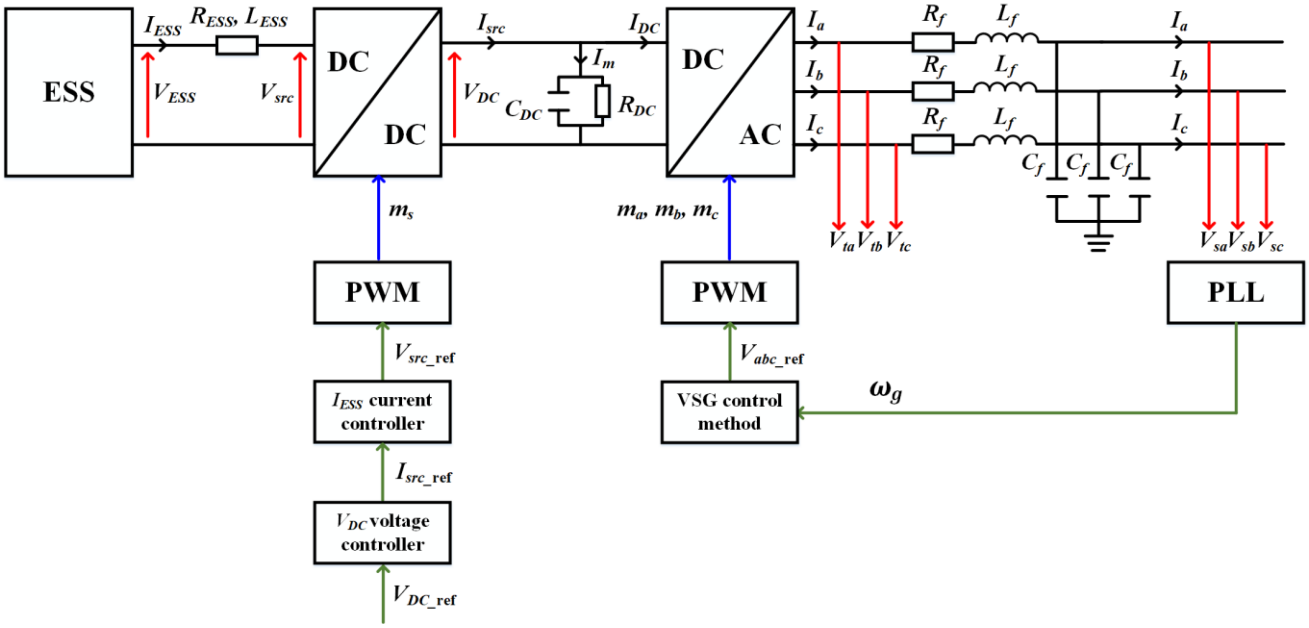

Fig. 8. Control scheme for HESS

the optimal operating voltage range for a SC is typically from 50% to 97.5% of V_{scnom}.

$$\Delta E_{sc} = P_{max} \cdot t \tag{19}$$

and E_{sc} refers to the energy difference between two states within a time interval of t (seconds). It is assumed that P_{max} is determined for the worst-case scenario where the renewable energy source, in this case a PV system, is completely out of power.

For the EVs battery, the capacity needed for the Microgrid can be calculated as shown [26]:

$$C_{bat} = 1.5\frac{P_{max}t_{max}}{\eta} \tag{20}$$

where P_{max} and t_{max} respectively represent the maximum power and the response time that ensures the stability of the battery system. η denotes the charge/discharge efficiency of the battery. For electric vehicles using Lithium-ion polymer batteries, the efficiency η is 0.9 [27].

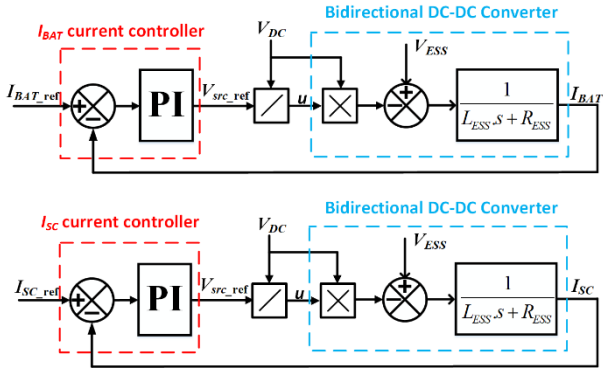

Fig. 9. Hybrid storage system current closed-loop control scheme

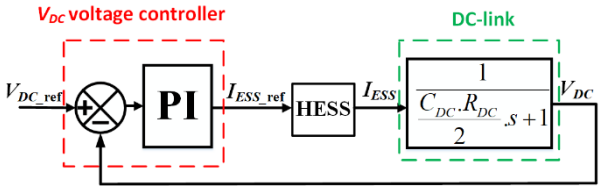

Fig. 10. DC voltage closed-loop control scheme

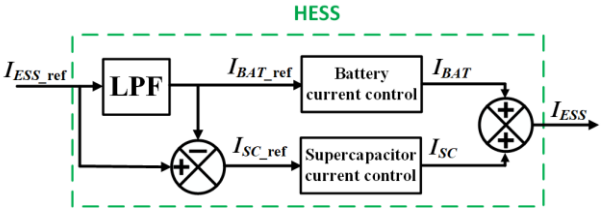

Fig. 11. Block diagram for current dividing and controlling of HESS

6 Simulation

In this paper, the structure of microgrid illustrated in Fig. 1 will be chosen for simulation. Furthermore, the Microgrid operates exclusively in islanded mode. The chosen values for the DC and AC bus voltages are 1000 V and 0.4 kV, respectively. In the PV system, the power output of the DC/DC boost converter will vary according to the assumed solar radiation fluctuations depicted in Fig. 12 using the MPPT P&O algorithm. Accordingly, the first and last stages in the scenario represent the PV system reaching its maximum power output at a radiation level of 1000 W/m^2, while the middle stage represents the system's power output decreasing to a minimum of 300 W/m^2 due to objective reasons (e.g., solar panel shading, malfunctions, etc).

Meanwhile, the load-changing scenario involves decreasing the initial power output by 10%, increasing it by 10%, and increasing it by 20% at the time intervals of seconds 30 to 80, seconds 100 to 120, and seconds 235 to 250, respectively, as depicted in Fig. 13. the load variation can be considered as a step function, from there evaluating the instantaneous response of the SC system. The simulation process will be performed for a 200 kWp PV system.

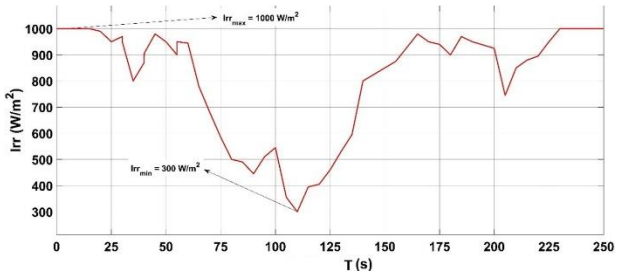

Fig. 12. Solar radiation scheme

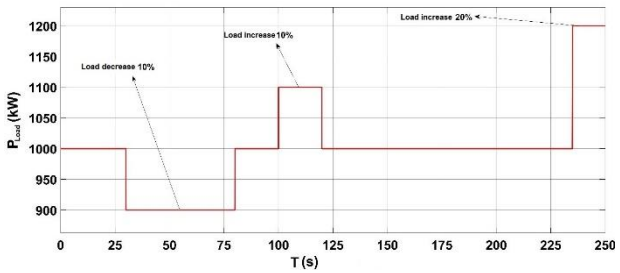

Fig. 13. Load demand curve

Table 1. Supercapacitor parameters

Parameters	Value of 1 module	Value SC system
Capacitance (C_{SC})	165 F	12.69 F
Series resistance (R_{sSC})	6.3 mΩ	81.9 mΩ
Parallel resistance (R_{pSC})	86.625 Ω	1126.1 Ω
Rated voltage (V_{SC})	48 V	624 V

6.1 HESS parameters

From formula (18), the capacitance can be calculated with V_{nom}=600V, P_{max}= 400 kW, and t= 4 s. Therefore, the capacitance of the SC pack is C_{sc}=12.69 F.

The capacitor that will be used is a BMOD0165 P048 BXX model manufactured by Maxwell. When connected in series with 13 modules, the following specifications are obtained in TABLE I.

For the EVs battery, Hyundai's KONA Electric Vehicle will be used for simulation, with a capacity of 64 kWh. From Eqn. (20), the capacity needed for the microgrid with 200 kW PV with t_{max}=1 s is 333 kWh. With the required capacity and type of vehicle, the minimum quantity of electric vehicles parked that are connected to participate in the electrical system regulation is 333/64 = 6 cars. Assume that the initial SoC of 6 EVs is 50%.

6.2 Synchronous generator parameters

The parameters of the synchronous generator are represented as shown in Tab. 2.

Table 2. Synchronous generator parameters

Parameters	Value
Rated Power (P_{nom})	1.8 MW
Rated voltage (V_{nom})	0.4 kV
Rated frequency (f_{nom})	50 Hz
Response time (T_{diesel})	1 s
Slope coefficient (s_{SG})	0.06 (6%)

The role of the diesel generator in the Microgrid is to serve as a baseload power source and contribute partly to the primary frequency regulation process when oscillations occur, especially in cases where there is no participation from the battery storage system of electric vehicles. Fig. 14 illustrates the dynamic model of a diesel generator, which is the most basic model comprising the primary frequency control stage as well as the delay caused by transmission systems, prime mover, and governor [28].

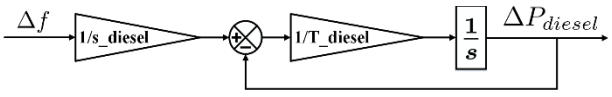

Fig. 14. Dynamic model of synchronous generator

6.3 Simulation result

Scenario 1: *Storage system in EVs is utilised*. As seen in Fig. 15, the continuous fluctuations of solar energy will be compensated by the power of the battery storage system in EVs, thereby maintaining a stable DC voltage at the DC bus. The power of each EV depends on its SoC, and is calculated from the formula in (17). The instantaneous change of the AC bus power will be carried by the SC system when the load changes instantaneously.

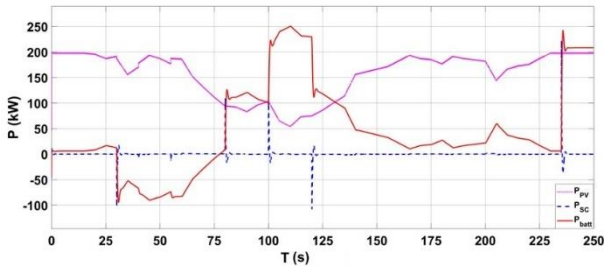

Fig. 15. Active power at DC Bus in case 1

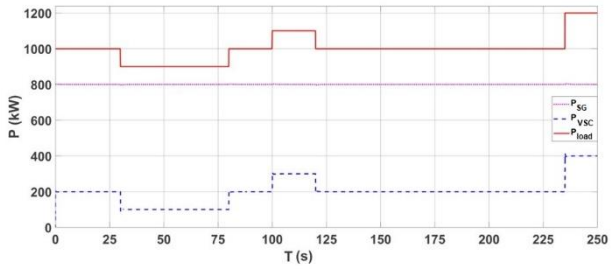

Fig. 16. Active power at AC Bus in case 1

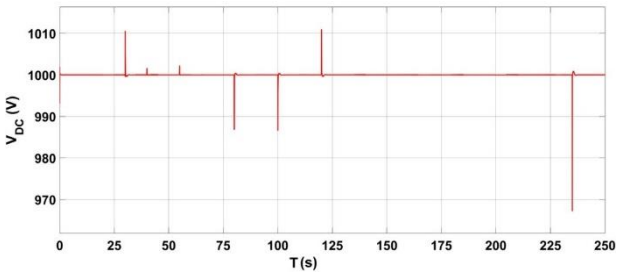

Fig. 17. DC bus voltage in case 1

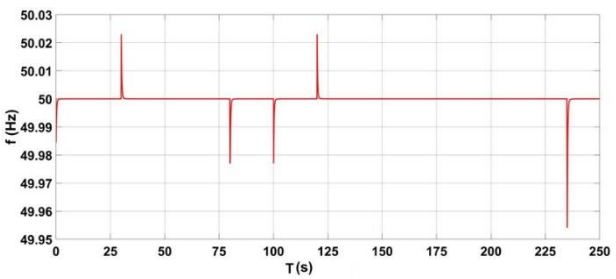

Fig. 18. Microgrid frequency response in case 1

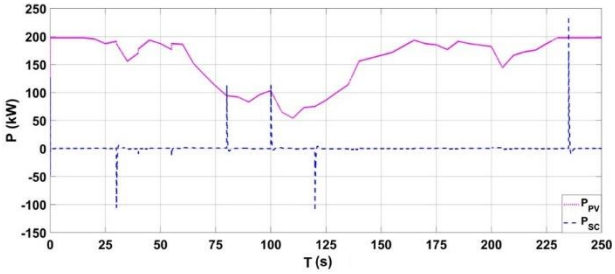

Fig. 19. Active power at DC bus in case 2

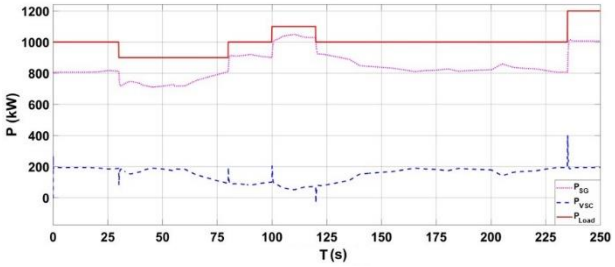

Fig. 20. Active power at DC bus in case 2

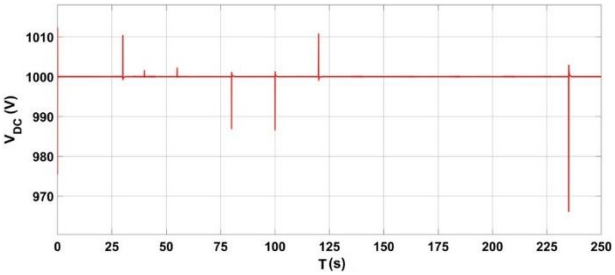

Fig. 21. DC bus voltage in case 2

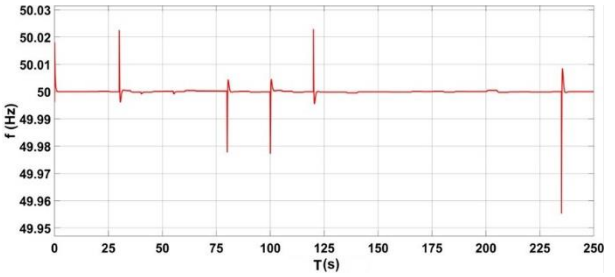

Fig. 22. Microgrid frequency response in case 2

There are still overshoots in DC voltage and frequency whenever the load changes immediately, because of the excess or lack of power source on the DC bus. Especially when the load increases by 20%, the response of the DC voltage change is 30 V, equivalent to 3% of the rated value as shown in Fig. 17. Regarding the system frequency in Fig. 18, the oscillation of the PV source almost does not affect the frequency oscillation. When electric vehicles are integrated into the system, the diesel generator's output barely changes (almost unchanged if the power demand of the load stays constant). Therefore, the participation of electric vehicle systems will reduce the operating costs of the synchronous generator.

<u>*Scenario 2*</u>: *When storage system in EVs is not utilised.* Similarly to scenario 1, results of this case are also shown in Figs. 19 to 22.

In the absence of electric vehicle participation, the synchronous generator will regulate the generated power in response to changes in solar energy. Similarly to

scenario 1, the SC system, as shown in Fig. 19, only varies with large frequency power fluctuations (mostly due to load changes and a small part due to the PV system) according to the above calculation formula and will quickly reach steady state (without charging/discharging). Thus, the computed capacity required for the SC system is not excessively high, which lowers the cost of investment. As for V_{DC} voltage, the overshoot (its reason is explained above) in this scenario is larger than that of the 1st scenario.

Comparison: Figure 23 compares the DC voltage in the two scenarios. For the frequency shown in Fig. 24, the absence of electric vehicles (EVs) causes small fluctuations due to the variations in the PV source. However, sudden load changes result in a larger overshoot without EV participation. In general, the frequency is stabilized with fewer large oscillations thanks to the response of the SC system over a short period. Figure 25 compares the synchronous generator's output power with and without EV participation. It can be seen that the settling time of frequency response when having EV is shorter and less damping compared to when there is no EV intervention. Compared to the first scenario, the synchronous generator output power in the 2nd scenario of not utilising EV's storage must continuously adapt to the solar source's fluctuations. Therefore, when the synchronous generator has to provide continuous power over a short period, it increases operational costs and reduces the generator's lifespan and efficiency.

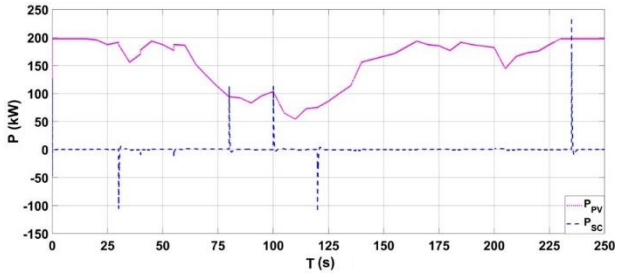

Fig. 23. Comparison of V_{DC} voltage response in scenarios 1 and 2

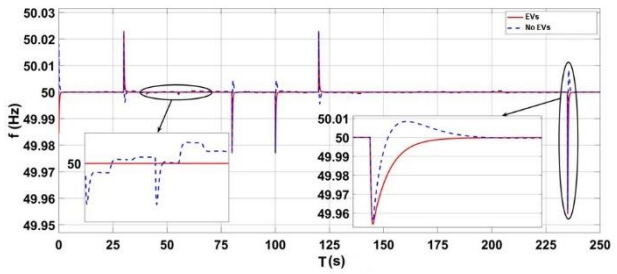

Fig. 24. Comparison of microgrid frequency response in scenarios 1 and 2

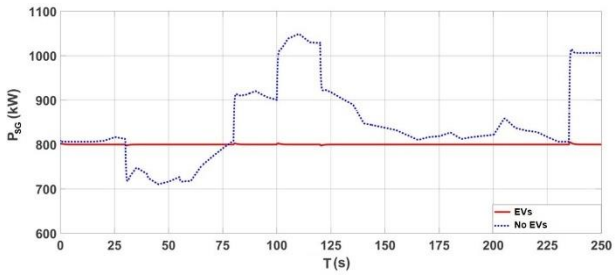

Fig. 25. Comparison of SG active power in cases 1 and 2

With this configuration, the larger the number of EVs participating in grid support, the less dependence on SG and PV system in times of little or no solar radiation. Because the large storage system of EVs will compensate for that capacity shortage. The major role of diesel generators in microgrids can be reduced by enhancing the participation of distributed energy resources as well as implementing V2G storage systems, thereby reducing maintenance costs and fuel expenses for the generators.

7 Conclusion

Amid the increasing penetration of renewable energy sources into the power system, especially solar energy, instability in frequency and voltage within the grid has become a concern due to the uncertain nature of these sources. The integration of energy-storage systems (ESS) is one of several strategies meant to improve the integration of renewable energy sources and maintain system stability. Additionally, applying the VSG control method to PV + HESS systems can simulate the characteristics of a synchronous generator to ensure stability and increase the penetration capability of PV sources. However, investing in an energy storage system can be costly.

This paper highlights the potential of electric vehicles (EVs) beyond transportation, as they can serve as storage systems when connected to the grid, helping to reduce fluctuations in uncertain renewable energy sources and relieve the burden on existing power sources in the system, such as synchronous generators. The combination of batteries and supercapacitors forms a hybrid storage system with high energy density and power density. Supercapacitors provide fast charging and discharging capabilities for instantaneous power fluctuations, while batteries offer long-term energy storage to maintain stable power output after transient processes.

Simulation results using Matlab/Simulink software demonstrate the effectiveness of the storage system combining electrochemical batteries in EVs and supercapacitors, along with the virtual synchronous generator (VSG) control method. As a result, integrating inertial-less and non-regulating distributed generation

sources (such as solar energy) into the power system becomes easier.

Future research directions involve refining the VSG control model, and further evaluating and analyzing the potential and role of EVs. Additionally, a more detailed assessment is needed to optimize the required storage capacity and supercapacitor sizing in the system to ensure cost-effective investments for future microgrids.

Acknowledgements

This work was supported by The Murata Science Foundation and The University of Danang, University of Science and Technology, code number of Project: T2023-02-06MSF.

References

[1] A. Ulbig, T. S. Borsche, and G. Andersson, "Analyzing rotational inertia, grid topology and their role for power system stability", *IFAC-PapersOnLine*, vol. 48, no. 30, pp. 541-547, 2015. doi:10.1016/j.ifacol.2015.12.436

[2] V. T. Nguyen, T. B. T. Truong, Q. T. Tran, C. Hoang, V. Q. V. Tran, M. T. Nguyen, "Vehicle-to-grid application to improve microgrid operation efficiency", *Measurement, Control, and Automation*, vol. 3, no. 2, pp. 75-81, Nov. 2022.

[3] H. Bevrani, *Robust power system frequency control*, Cham: Springer, 2014.

[4] D. Groß, S. Bolognani, B. K. Poolla, and F. Dörfler, "Increasing the resilience of low-inertia power systems by virtual inertia and damping", *Proceedings of IREP'2017 Symposium*, pp. 64-75, 2017.

[5] Z. Lu, M. Li, and J. Wang, "Virtual synchronous generator control strategy based on improved inner loop applied to power storage converter", *2019 IEEE 3rd International Electrical and Energy Conference (CIEEC)*, pp. 2055-2059, 2019.

[6] L. Ruttledge and D. Flynn, "Emulated inertial response from wind turbines: Gain Scheduling and Resource Coordination", *IEEE Transactions on Power Systems*, vol. 31, no. 5, pp. 3747-3755, 2016. doi:10.1109/tpwrs.2015.2493058

[7] A. Engler and N. Soultanis, "Droop control in LV-Grids", *2005 International Conference on Future Power Systems*, pp. 6-pp, 2005. doi:10.1109/fps.2005.204224

[8] B. Zhang, X. Yan, and S. Y. Altahir, "Control design and small-signal modeling of multi-parallel virtual synchronous generators", *2017 11th IEEE International Conference on Compatibility, Power Electronics and Power Engineering (CPE-POWERENG)*, pp. 471-476, 2017. doi:10.1109/cpe.2017.7915217

[9] Y. Chen, R. Hesse, D. Turschner, and H.-P. Beck, "Improving the grid power quality using virtual synchronous machines", *2011 International Conference on Power Engineering, Energy and Electrical Drives*, pp. 1-6, 2011. doi:10.1109/powereng.2011.6036498

[10] J. Chen and T. O'Donnell, "Analysis of virtual synchronous generator control and its response based on transfer functions", *IET Power Electronics*, vol. 12, no. 11, pp. 2965-2977, 2019. doi:10.1049/iet-pel.2018.5711

[11] D. Lauinger, F. Vuille, and D. Kuhn, "A review of the state of research on vehicle-to-grid (V2G): Progress and barriers to deployment", *Proceedings of European Battery, Hybrid and Fuel Cell Electric Vehicle Congress*, Geneva, 2017.

[12] W. Kempton and J. Tomić, "Vehicle-to-grid power implementation: From stabilizing the grid to supporting large-scale renewable energy", *Journal of Power Sources*, vol. 144, no. 1, pp. 280-294, 2005. doi:10.1016/j.jpowsour.2004.12.022

[13] J. A. Lopes, F. J. Soares, and P. M. Almeida, "Integration of electric vehicles in the Electric Power System", *Proceedings of the IEEE*, vol. 99, no. 1, pp. 168-183, 2011. doi:10.1109/jproc.2010.2066250

[14] R. T. Meyer, R. A. DeCarlo, and S. Pekarek, "Hybrid model predictive power management of a battery-supercapacitor electric vehicle", *Asian Journal of Control*, vol. 18, no. 1, pp. 150-165, 2015. doi:10.1002/asjc.1259

[15] S. Aragon-Aviles, A. H. Kadam, T. Sidhu, and S. S. Williamson, "Modeling, analysis, design, and simulation of a bidirectional DC-DC converter with integrated snow removal functionality for solar PV Electric Vehicle Charger Applications", *Energies*, vol. 15, no. 8, p. 2961, 2022. doi:10.3390/en15082961

[16] N. V. Tan, N. B. Nam, N. H. Hieu, L. K. Hung, M. Q. Duong, and L. H. Lam, "A proposal for an MPPT algorithm based on the fluctuations of the PV output power, output voltage, and control duty cycle for improving the performance of PV systems in Microgrid," *Energies*, vol. 13, no. 17, p. 4326, 2020. doi:10.3390/en13174326

[17] B. Bendib, H. Belmili, and F. Krim, "A survey of the most used MPPT methods: Conventional and advanced algorithms applied for Photovoltaic Systems", *Renewable and Sustainable Energy Reviews*, vol. 45, pp. 637-648, 2015. doi:10.1016/j.rser.2015.02.009

[18] Q. L. Lam, "Advanced control of microgrids for frequency and voltage stability: robust control co-design and real-time validation", *Ph.D. dissertation*, Université Grenoble Alpes, 2018.

[19] A. Yazdani, and R. Iravani, *Voltage-sourced converters in power systems: modeling, control, and applications*. Cham: John Wiley & Sons, 2010.

[20] S. D'Arco, J. A. Suul, and O. B. Fosso, "Small-signal modeling and parametric sensitivity of a virtual synchronous machine in islanded operation", *International Journal of Electrical Power & Energy Systems*, vol. 72, pp. 3-15, 2015. doi:10.1016/j.ijepes.2015.02.005

[21] H. V. P. Nguyen, B. N. Nguyen, T. B. T. Truong, H. D. Dao, Q. C. Le, "Stability Analysis of an islanded Microgrid using Supercapacitor-based Virtual Synchronous Generator", *2020 5th International Conference on Green Technology and Sustainable Development (GTSD)*, pp. 454-460, Ho Chi Minh City, Vietnam, 2020. doi:10.1109/gtsd50082.2020.9303070

[22] P. Tielens and D. V. Hertem, "The relevance of inertia in power systems", *Renewable and Sustainable Energy Reviews*, vol. 55, pp. 999-1009, 2016. doi:10.1016/j.rser.2015.11.016

[23] S. Hajiaghasi, A. Salemnia, and M. Hamzeh, "Hybrid energy storage system for Microgrids Applications: A Review", *Journal of Energy Storage*, vol. 21, pp. 543-570, 2019. doi:10.1016/j.est.2018.12.017

[24] S. U. Khan, K. K. Mehmood, Z. M. Haider, S. B. A. Bukhari, S. J. Lee, M. K. Rafique, and C. H. Kim, "Energy Management Scheme for an EV smart charger V2G/G2V application with an EV power llocation technique and voltage regulation", *Applied Sciences*, vol. 8, no. 4, p. 648, 2018. doi:10.3390/app8040648

[25] N. Mendis, K. M. Muttaqi, and S. Perera, "Active power management of a super capacitor-battery hybrid energy storage system for standalone operation of DFIG based wind turbines", *2012 IEEE Industry Applications Society Annual Meeting*, pp. 1-8, 2012. doi:10.1109/ias.2012.6374045

[26] N. H. Hieu, N. V. Tan, N. B. Nam, T. D. M. Duc, D. H. Dan, and L. Q. Cuong, "The Roles of Energy Storage Systems in Stabilizing Frequency of the Islanded Microgrid", *The University of Danang - Journal of Science and Technology*, vol. 18, no. 5, pp. 39-44, 2020.

[27] U. Akram, M. Nadarajah, R. Shah, and F. Milano, "A review on rapid responsive energy storage technologies for frequency regulation in modern Power Systems", *Renewable and Sustainable Energy Reviews*, vol. 120, p. 109626, 2020. doi:10.1016/j.rser.2019.109626

[28] M. Datta, H. Ishikawa, H. Naitoh, and T. Senjyu, "Frequency control improvement in a PV-diesel hybrid power system with a virtual inertia controller", *2012 7th IEEE Conference on Industrial Electronics and Applications (ICIEA)*, pp. 1167-1172, 2012. doi:10.1109/iciea.2012.6360900

Received 1 September 2023